Revisiting the Mechanical Limited-Slip Differential for High-Performance and Race Car Applications

Marco Gadola, Daniel Chindamo, and Basilio Lenzo, *Member, IAENG*

***Abstract*— This paper provides a comprehensive revision of the working principles and limitations of the mechanical limited-slip differential (LSD), a passive device used to improve traction capabilities and to extend the performance envelope of high-performance road cars, racing and rally cars. The LSD has been in use for decades. However, according to the authors' experience, its impact on vehicle dynamics appears to be somewhat neglected in the literature and often misunderstood, especially in the semi-pro racing community. Current research on the subject is usually focused on side aspects and/or on modern control applications such as active differentials and torque-vectoring systems. These state-of-the-art technologies still rely on the same principles of the LSD, which should therefore be fully explained. The authors intend to fill this gap by starting with a comprehensive literature review. Then, an intuitive explanation of the impact of limited slip systems on vehicle behaviour is proposed with simple mathematical models and examples to integrate what seems to be missing. The peculiar shape of the torque-sensitive LSD working zone on the torque bias diagram is explained to an unprecedented level of detail. Real-world application examples are provided, including data recorded on a single-seater racecar integrated with examples based on a virtual model.**

***Index Terms*— limited slip differential, vehicle dynamics, vehicle stability, torque bias diagram, yaw moment control.**

NOMENCLATURE

AWD, 4WD: All Wheel Drive, Four Wheel Drive

FWD, RWD: Front Wheel Drive, Rear Wheel Drive

RWS, 4WS: Rear Wheel Steering, Four Wheel Steering

a_y: lateral acceleration

c: track width, drive axle

C_m: differential input torque

$C_{1,2}$: output torque at each wheel

Manuscript received Oct 2, 2020; revised Mar 07, 2021.

M. Gadola is an Associate Professor of Mechanical Enginering at the University of Brescia, Dipartimento di Ingegneria Meccanica e Industriale, 25123 Brescia, Italy (e-mail: marco.gadola@unibs.it).

D. Chindamo is a Researcher of Mechanical Enginering at the University of Brescia, Dipartimento di Ingegneria Meccanica e Industriale, 25123 Brescia, Italy (e-mail: daniel.chindamo@unibs.it).

B. Lenzo is a Senior Lecturer in Automotive Engineering at Sheffield Hallam University, Department of Engineering and Mathematics, S11WB Sheffield, UK (corresponding author phone: +44 0114 225 3747; e-mail: basilio.lenzo@shu.ac.uk).

ΔC : differential locking or torque transfer across the differential

C_{clutch}: torque capacity of the clutch pack

δ: steering angle (front axle only)

F_A: axial thrust on clutch pack

$F_{X1,2}$: longitudinal tyre force

ΔF_X: longitudinal tyre force difference across the axle

ΔF_Z: lateral load transfer

k: constant for additional locking effects

LSD, ALSD: Limited Slip Differential, Active LSD

m: vehicle mass

μ: friction coefficient, tyre contact patch on road surface

μ_C, μ_S, μ_D: generic friction coefficient, clutch pack disks; static and dynamic friction coefficient

μ_R: friction coefficient between pin and ramp surface

M_Z: yaw moment

N, N_T, N_A: forces exchanged between gear pin and ramp: normal force, tangential and axial components

n: number of clutch disk interfaces (per side)

P (P-): generic preload torque (negative preload torque)

PTVD: Passive Torque Vectoring Differential

$\dot{\psi}$: yaw rate

r: tyre rolling radius

R: cornering radius

R_0, r_i: inner and outer radius of clutch pack disc

r_{ramp}: ramp radius

$S_{1,2}$: longitudinal tyre slip or slip ratio

σ: ramp angle

V: vehicle forward speed

VCP: Viscous Coupling Plate

ω_m: angular velocity, final drive

$\omega_{1,2}$: angular velocity of each wheel

$\Delta\omega$: angular velocity difference across the differential or viscous coupling

W_P: power loss across the differential

TB, TB%: Torque Bias ratio

TCS, ABS, ABC: Traction Control System, Anti-lock Braking System, Active Brake Control

SUBSCRIPTS
1, 2: LEFT- AND RIGHT-HAND WHEEL

I. INTRODUCTION

Differential (diff) locking can help to solve traction problems on low friction surfaces. On high-performance vehicle applications with a high power-to-weight ratio it can also help to improve cornering behaviour and stability through the development of a yaw torque with a direct impact on handling characteristics.

Passive LSD devices are usually classified as speed-sensitive (a locking torque is developed as a function of wheel speed difference, where a viscous cartridge is fitted in parallel with an open differential for instance) or torque-sensitive, where the locking action is proportional to input torque: the so-called ramp or Salisbury differential for instance. These devices are now superseded by actively controlled differentials or even by torque vectoring systems, where not only the magnitude but also the direction of torque transfer across the differential is under control. However active systems are expensive and require deep system knowledge, integration with the other chassis control systems and very careful tuning to be effective. On the contrary the use of traditional, passive, torque-sensitive differentials is still widespread where a back-to-basics driving experience is the key to marketing success, such as on lightweight sports cars. Active systems moreover are often banned even in professional motorsport in order to limit costs and keep complexity under control. In these cases, traditional LSDs are the standard: examples are all the various "road to Formula 1" championships like Formula 2 and Formula 3 and also Touring, Grand Touring and Endurance racing. However, according to the authors' experience as trackside engineers, the LSD is still a fairly unknown item, although its impact on vehicle performance is significant. Torque sensors are expensive and not very robust, hence usually output torque signals are not available in the data acquisition system, and this is probably one of the reasons. The experimental work described in [1] is one of very few evidences of a testing campaign dedicated to LSD characterization in motorsport.

A literature survey over more than 40 years of research resulted in just a few papers dealing with the passive LSD, while the topic is probably considered too specific even for the mainstream literature on the subject of vehicle dynamics. Needless to say, some of the works now appear slightly out of date. For example [2] is a “historic” American paper focused on the traditional live axle suspension, dealing with the principles of the torque-sensitive action on a basic differential coupled with a clutch pack. The authors do not mention the impact of the system on handling and deal solely with the traction problem. The paper introduces useful definitions like the torque bias ratio, and describes an arrangement for a test rig dedicated to the so-called μ-*split* condition, i.e. where the wheels on one side of the car are on a low-grip road surface and a yaw moment arises in acceleration. An early evidence of an experimental campaign conducted by a major manufacturer is [3], describing a comparison of free vs fully locked vs viscous vs ramp differential in terms of traction, braking and handling, including steady-state steering pad testing, throttle-off manoeuvers and frequency response analysis. An oft-quoted work is [4], written by Gleason Corporation to promote their patented torque-sensitive LSD concept called *Torsen*®. The traction problem is dealt with extensively but the impact of torque bias on handling is not mentioned. An overview of conventional LSD systems is mainly aimed at highlighting their disadvantages. A somewhat similar work is [5], introducing the *Gerodisc*® system for racing applications. This is mainly a passive hydro-mechanical coupling that can achieve speed-sensitive and/or torque-sensitive differential locking action. Although a bit contradictory, [6] is an interesting paper written by Nissan engineers showing that a viscous coupling on a RWD car can work in conjunction with a TCS, the former working for low slip values and the latter coming into play in the high slip region. Traction, handling, stability, and system architecture are examined. A very interesting read is [7], a paper written by GKN to describe pros and cons of passive LSDs on high-power FWD cars. The influence of standard and progressive speed-sensitive devices and torque-sensitive units on vehicle behaviour and driver workload is tested. The interaction of torque biasing with steering geometry and suspension elasto-kinematics is also investigated. A comprehensive experimental analysis on the behaviour of RWD cars equipped with a LSD is in [8]. The study is validated through a testing campaign, distinguishes between preload and ramp contributions, takes transmission inertia effects into account during transients. The authors also state that the overall suspension setup should be tuned according to the influence of the LSD on vehicle behaviour. However, the torque bias diagram is not dealt with, the traction problem is just mentioned, and somehow basic conclusions are given. Despite being universally considered the best reference for the dynamics of high-performance and racing cars, [9] deals with limited slip differentials very quickly in Section 20.2 and reports the peculiar shape of the ramp differential working zone in a torque bias diagram without any explanation, probably leaving the average reader with some open questions. The featured LSD characteristics, for example, have a symmetric behaviour on and off power, which is usually not the case in real-world applications. Among the most renowned books on vehicle dynamics, apparently [10] is the only one dealing extensively with LSDs and their impact on handling. Unfortunately, the beneficial effect in terms of stability off-power is totally missed as torque-sensitive systems are said to "act as free differentials on the overrun".

Celebrated Formula 1 engineer Peter Wright [11] introduces the principles of torque vectoring with an intelligible explanation, but the basics of the LSD are not described. [12] is an analysis of the steady-state behaviour of a vehicle with a fully locked differential i.e. with a so-called "spool" by means of a very detailed although simplified numerical model. Practical implications however are basically neglected and the study is mainly theoretical. A relevant work, entirely focused on the mechanical LSD, is [13]: detailed modelling of the ramp differential internals is used to match a theoretical locking model with experimental

data (see Section 3.5). The wedging action of the ramps is supplemented by other forces and inherent friction between moving parts.

Recent works by Tremlett *et al.* are focused on the impact of passive LSD devices on the handling and performance envelope limits of either FWD and RWD racing cars. [14] combines both a torque-sensitive and a speed-sensitive device in a so-called VCP (Viscous Combined Plate) diff on a FWD car and uses a comprehensive model to simulate significant manoeuvers. Although this work is a relevant contribution to the subject, the authors do not underline what is perhaps considered an obvious statement: the performance of a FWD racing car is inherently limited by poor traction due to longitudinal load transfer on power and to high force demands on the front wheels, therefore a torque-sensitive device alone is not very effective, and preload is detrimental to performance because it further increases understeer, steering activity, and driver workload. [15] basically extends the scope of [14] to a theoretical Passive Torque Vectoring Differential (PTVD) guided by a functional characteristic similar in shape to tyre saturation curves. [16] is one of very few papers to go "back to basics": it explains the typical shape of the mechanical LSD locking action. Experimental tests performed on a dedicated rig support the explanations. The conclusions basically confirm the different effects on handling balance, stability, and traction, that are also well explained by Cheli in [17]. Tremlett's work also extends to modelling and simulation of semi-active differential systems. [18] applies the theory of optimal control to a RWD racing car model performing a double-lane change manoeuver. It is a sort of "blind approach" to the optimization of a hypothetical, speed-sensitive differential featuring an active, variable-response characteristic. Dal Bianco *et al.* also apply optimal control theory to the simulation of an entire race lap with the model of a GP2 single-seater racecar equipped with a LSD in [19]. In [20] an in-depth description of the torque-sensitive LSD is provided with its effects on handling, also extending to a simplified representation of the torque bias diagram. The impact of the LSD on FWD cars in terms of the so-called torque steer is dealt with in [21].

Contemporary research is focused on active systems and assumes the basics of yaw control for granted. Among many papers, some that do recall the principles of a passive LSD are listed hereinafter. [22] for instance explains the torque-sensitive LSD by means of a simplified diagram. A very useful contribution is [23], describing the criteria used to design the control strategy of the active limited-slip differential adopted on Ferrari sportscars about ten years ago, with the related advantages in terms of handling and stability. Guidelines for tuning a passive LSD can be drawn as well, where the action required is clearly split into three different situations according to driver demand, vehicle state and road conditions: steady state/power on, power off, and pure traction/μ-*split*. An understeer curve (steering angle δ vs lateral acceleration) is also traced for generical open, limited-slip and semi-active differentials on the same car. The active LSD is also the subject of [24], a fairly recent study based either on the traditional single-track vehicle model with linear tyres, and on a more complex model built within the *CarSim*® software. Yaw stability is controlled by means of model predictive control theory [25-26] applied to the ALSD.

Although active control is beyond the scope of this paper, the following works are proposed for a further look into models and systems for yaw dynamics and control. For instance [27] describes a model for the internal dynamics of a "steering differential" which is the typical torque-vectoring system based on a counter-rotating side shaft. [28] proposes an interesting and well-structured comparison between an electronically controlled LSD, an ideal torque vectoring system and a real-world one by means of a traditional vehicle dynamics model. The most interesting concept is about torque vectoring. The system, also enabling torque transfer from the slower to the faster wheel [29], is inherently more suitable to modify vehicle balance by reducing understeer (or even by generating oversteer) than the opposite, due to potential saturation of the inner tyre on power. Again from Hancock [30] is an interesting comparison between the potentials of torque vectoring and active brake control systems to improve the yaw-sideslip handling characteristics of a high-performance RWD car. Energy requirements are also discussed. Although the authors classify this work as a preliminary investigation, the conclusions state that the systems can be complementary, but the ABC should be mainly used to reinstate driver control in emergency situations only. Nowadays it is well-known that brake intervention as a primary measure to influence vehicle cornering behaviour is considered undesirable. A comparison of different torque vectoring systems can also be found in [31]. More on active yaw control can be found in [32-42]. Here estimated states such as vehicle speed or sideslip angle [43] are often required. Some works deal with the comparison of an active differential vs RWS for yaw moment control. Two examples covering a large time span are [44-45], while also active front wheel steering is dealt with in [46]. Papers dealing with active differentials based on electro-rheological fluids are [47-48]. The latter is a comprehensive study based on the *CarSim*® software. Although the shortcomings of a passive LSD are used as a baseline for the development of the ALSD control strategy, apparently the paper is in contrast with similar ones like [23] and some degree of perplexity inevitably arises. For the sake of completeness, it should be noted that [9] classifies LSD adjustment as a secondary setup item in racing. Nowadays the diff is generally considered a primary one, while other factors should be added to the list of the secondary items, like suspension and steering friction [49-50], the interaction between vertical and lateral loads in the steering system [51], as well as the coupling between suspension non-linearities and downforce [52]. Again, although the LSD can also play a role in driverless experimental vehicles [53] its impact on driver workload can be a key to performance [54]. Last but not least, along this literature survey a progressive shift from proving ground testing with real-world vehicles to vehicle dynamics numerical models to control theory is evident. A further shift towards Human-in-the Loop testing on driving simulators is already in progress and will certainly become even faster in the next few years.

This work is intended to provide a clear and comprehensive explanation of how a typical passive LSD works and how it affects vehicle behaviour by using math models and examples, with the aim of filling the gap encountered in the related literature.

II. BASIC PRINCIPLES

A. Tyre characteristics: longitudinal and combined forces

As it is always the case in vehicle dynamics, a good knowledge of tyre characteristics is required to understand how the LSD affects vehicle behaviour. The typical shape of pure traction/braking force vs longitudinal slip and combined lateral and longitudinal forces are recalled in this section. A practical definition of the longitudinal slip is the slip ratio

on power: $S = \frac{\omega r - V}{\omega r}, \quad 0 \leq S \leq 1$ (1)

off power: $S = \frac{\omega r - V}{V}, \quad -1 \leq S \leq 0$ (2)

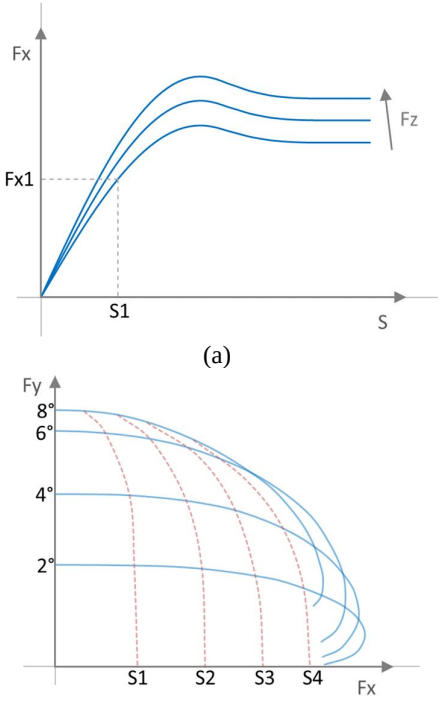

Figure 1. a) longitudinal force vs slip, b) combined slip curves: lateral vs longitudinal force on power.

The longitudinal force vs slip curve is shown in Figure 1a. Only positive values (on power) are shown, assuming the negative slip curve is symmetric. For a given vertical load an almost linear zone is followed by a peak around $S \approx 0.1$ then a strongly non-linear zone called saturation occurs: the tyre is not able to give further increments in terms of tractive force, as adhesion is superseded by slippage along the whole length of the tyre contact patch. The curves are scaled up for increasing vertical load, considering non-linear effects due to load sensitivity as negligible [55,20].

Figure 1b, showing the so-called combined case, highlights the strong interaction between the development of lateral and longitudinal forces on a single tyre at the same time, once again for a given vertical load [55].

B. The spool: basic axle with no or locked differential

The simplest form of final drive is the so-called spool. If there is no differential and the left and right drive wheels are rigidly connected (like a kart), or if the differential is fully locked, both wheels are forced to rotate at the same angular velocity. The input power is equal to the output power and it is the same for the overall torque (see Figure 2a):

$\omega_m = \omega_1 = \omega_2 \qquad C_m = C_1 + C_2$ (3)

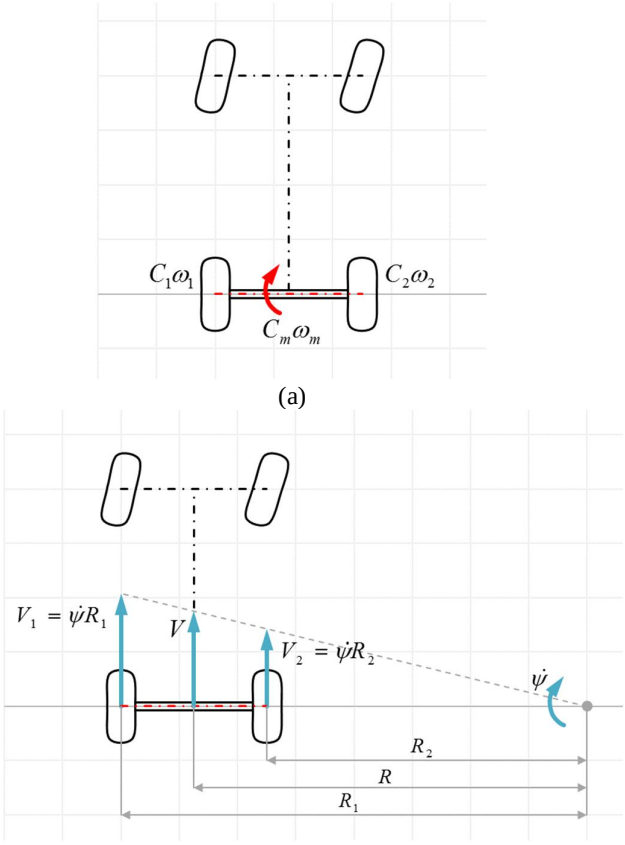

Figure 2. a) RWD car with spool axle, b) forward velocities of the driven wheels.

It is impossible however to calculate the torque distribution on the drive wheels (the so-called torque bias) without taking the longitudinal tyre force vs slip characteristics into account. In other words the tyres determine the torque bias, mainly according to longitudinal slip ratio and vertical load. For a given speed and a given cornering radius, therefore in steady-state turning, the forward velocities of the outer and inner wheels are dependent upon the track i.e. the wheel relative distance (Figure 2b):

$V_1 = \dot{\psi}R_1 \quad$ and $\quad V_2 = \dot{\psi}R_2$

with $R_1 = R_2 + c \quad$ and $\quad V = \dot{\psi}R$ (4)

The following sections are aimed at explaining the impact of the spool on vehicle balance, handling and stability in an intuitive manner. Some assumptions are used for simplicity: the effect of combined tyre slip is dealt with separately for instance. Tyres are assumed to work in the linear range of the longitudinal force vs slip curve i.e. before the onset of saturation. The rolling radius is considered equal on both sides of the drive axle, and second-order effects like the camber influence are not considered.

C. Steady state / on power cornering

According to the definition of longitudinal slip on power:

$$S_1 = \frac{\omega_1 r - \dot{\psi} R_1}{\omega_1 r} \qquad S_2 = \frac{\omega_2 r - \dot{\psi} R_2}{\omega_2 r}$$

$$\text{with} \quad \omega_m = \omega_1 = \omega_2 \tag{5}$$

The longitudinal tyre slip difference is determined by kinematics:

$$S_2 - S_1 = \frac{\omega_m r - \dot{\psi} R_2}{\omega_m r} - \frac{\omega_m r - \dot{\psi} R_1}{\omega_m r} =$$

$$= \frac{\dot{\psi}(R_1 - R_2)}{\omega_m r} = \frac{\dot{\psi} c}{\omega_m r} = \frac{Vc}{R \omega_m r} \tag{6}$$

Since $R_1 > R_2$ the inner wheel slip is larger hence $S_2 > S_1$. The slip difference is proportional to the track width and inversely proportional to the cornering radius. Now, assuming that lateral acceleration and lateral load transfer ΔF_Z are negligible, $F_{X2} > F_{X1}$ and a yaw moment is generated:

$$M_Z = \Delta F_X \cdot c = (F_{X2} - F_{X1}) \cdot c \tag{7}$$

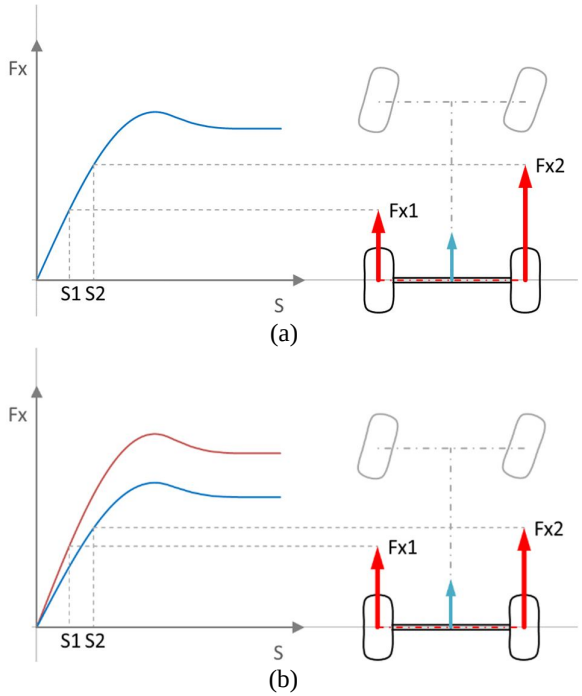

Figure 3. Yaw moment induced by spool. a) low-speed cornering, b) effect of lateral load transfer.

In agreement with [8,12], Figure 3a shows that the yaw moment on power is an understeer contribution. As this stabilizing effect is inversely proportional to the cornering radius it is particularly significant in tight cornering at very low speed, during a parking maneuver for instance: the spool will resist yaw rate therefore spoiling vehicle maneuverability, and friction at the contact patch will dissipate energy, causing premature tyre wear as well. When lateral acceleration is higher, the lateral load transfer ΔF_Z is no longer negligible (Figure 3b): the inner and outer tyres work on separate curves. The yaw moment is still towards understeer, but the amount is reduced.

Finally for extreme cornering speeds and very high lateral acceleration, the lateral load transfer causes the inversion of the yaw moment, that becomes an oversteer contribution (Figure 4a). On top of that when considering the combined tyre slip curves, a strong demand of tractive force will cause the outer wheel to shift towards higher slip angles (Figure 4b), thus further increasing the tendency to oversteer on a RWD car. This change in terms of vehicle balance can be unpredictable hence it is undesirable, unless a reasonable amount of understeer is built into the overall vehicle setup to take this effect into account properly. In other words a spool makes the handling balance strongly affected by lateral acceleration and torque demand, generating understeer for low a_y and oversteer –probably associated with poor stability- for a_y levels close to the cornering limit.

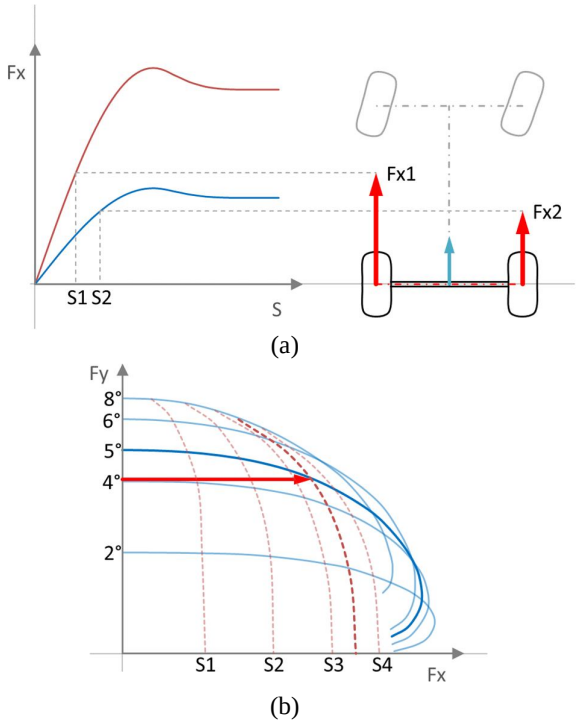

Figure 4. a) oversteer induced by spool in high-speed cornering, b) combined slip on rear outer tyre.

D. Off power behaviour

Releasing the throttle means that the drive tyres will develop negative longitudinal forces due to the engine braking torque. Once again assuming the same rolling radius on both axle sides and according to the definition of negative longitudinal slip, the slip difference is determined by kinematics:

$$S_1 = \frac{\omega_1 r - \dot{\psi} R_1}{\dot{\psi} R_1} \qquad S_2 = \frac{\omega_2 r - \dot{\psi} R_2}{\dot{\psi} R_2}$$

$$\text{with } \omega_m = \omega_1 = \omega_2 \tag{8}$$

$$S_2 - S_1 = \frac{\omega_2 r - \dot{\psi} R_2}{\dot{\psi} R_2} - \frac{\omega_1 r - \dot{\psi} R_1}{\dot{\psi} R_1} =$$

$$= \frac{\omega_m r}{\dot{\psi}} \left(\frac{R_1 - R_2}{R_1 R_2} \right) = \frac{\omega_m r}{\dot{\psi}} \left(\frac{c}{R_1 R_2} \right) \tag{9}$$

with $R_1 > R_2$ and $|S_1| > |S_2|$. When lateral acceleration and load transfer ΔF_Z are negligible, then $|F_{X1}| > |F_{X2}|$ and an understeer moment, resisting yaw, is generated (Figure 5a). In this case however even when lateral acceleration and load transfer are higher or extreme there is no inversion of the yaw moment, that remains on the understeer side (Figure 5b).

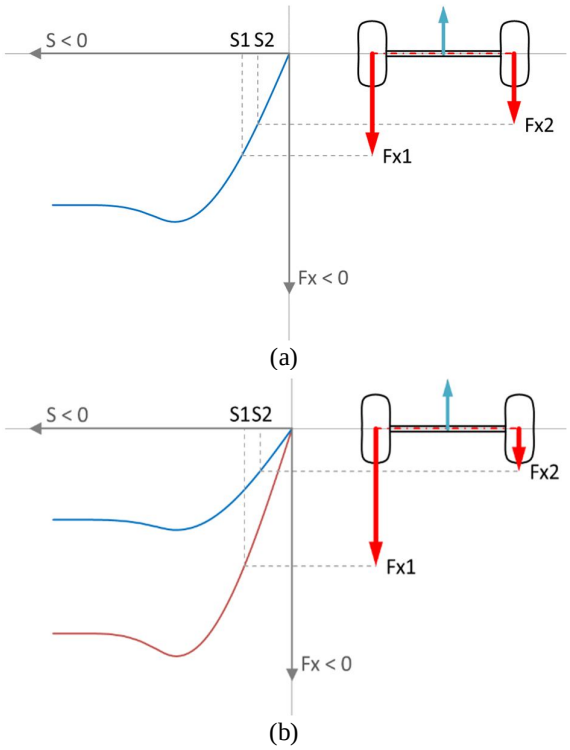

Figure 5. Spool effect off power. a) low-speed cornering, b) high-speed cornering.

Table 1. Yaw moment contribution induced by spool: effect on handling balance.

Cornering state	**Yaw moment**
Steady state, low speed	UNDERSTEER
On power, low a_y	UNDERSTEER
On power, high a_y	OVERSTEER
Off power, low a_y	UNDERSTEER
Off power, high a_y	

Generally speaking a spool or locked differential always resists vehicle yaw even at very low speed, and unless the vehicle is driven close to the cornering limits. In this case the high lateral load transfer coupled with the demand of large tractive forces can result in an abrupt change of vehicle balance towards oversteer and instability.

On the other side releasing the throttle in a corner is a critical situation for stability in itself, as the longitudinal load transfer helps the front axle to develop high lateral forces with smaller slip angles, while the opposite happens on the rear axle. In this case a locked differential always gives an understeer contribution promoting stability, sometimes at the expense of vehicle agility (Table 1). The yaw moment also increases yaw damping, as long as it is towards understeer [27].

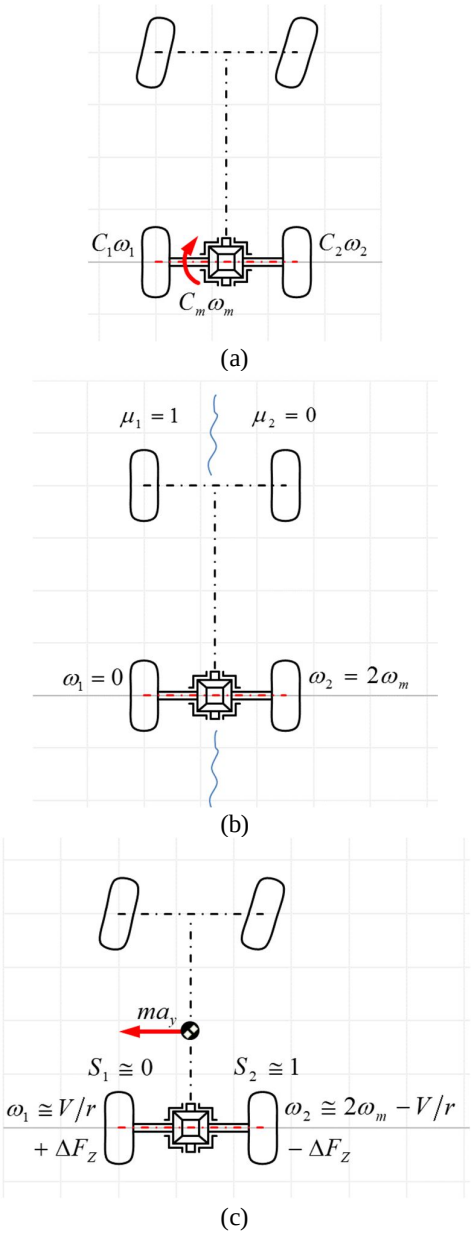

Figure 6. a) open differential. The traction issue: b) standing start on μ-*split*, c) high-speed cornering.

By the way a difference in longitudinal slip with the associated friction and consequently a yaw moment are also generated in straight running on an uneven road surface, or whenever tyre pressure and rolling radius are different between the drive wheels. All the above makes the spool hardly compatible with the requirements of a road vehicle.

E. The open differential

The open or free differential for modern automotive applications (Figure 6a) was patented by Monsieur Pecqueur in 1827. It is universally adopted on ground vehicles to decouple the angular velocities of the drive wheels, thus avoiding the undesirable side effects of a spool. The input torque C_m is transferred from the *differential carrier* to the pins of the *satellite bevel gears* to the *driven bevel gears*, which are coaxial and engaged with the output shafts.

Assuming that energy losses due to internal friction and inertial terms are negligible, a symmetric differential is fully described by the following equations:

$$C_m = C_1 + C_2 \quad \text{and} \quad C_1 = C_2 = C_m/2 \tag{10}$$

$$\omega_m = \frac{\omega_1+\omega_2}{2} \tag{11}$$

also known as *Willis' formula*.

The open differential can therefore deliver torque to both wheels that are free to rotate at different velocities, thus canceling tyre contact patch friction along a turn, and potentially achieving a condition close to pure rolling. The torque is always split into equal proportions left to right (once again neglecting internal friction) therefore, assuming the same rolling radius on both sides, there is no yaw moment either on and off power, and the transmission of torque does not interfere directly with vehicle handling, cornering balance and driver inputs. The output torque being equal on both sides, a traction problem however is encountered whenever one of the tyres saturates for any reason. Two typical situations can be taken as reference examples.

1) Standing start on a μ-*split* road surface: when a wheel is resting on a low-grip surface and can deliver limited or zero torque, neither this nor the other wheel can generate any torque/tractive force. In Figure 6b:

$$C_1 = C_2 = 0, \quad \omega_1 = 0, \quad \omega_2 = 2\omega_m \tag{12}$$

2) Accelerating in a corner with high lateral acceleration hence high lateral load transfer: the inner wheel tends to lift off the ground and the tyre can saturate, developing poor torque/tractive force. The same, limited amount of torque can be transmitted to the outer wheel. When the inner wheel is no longer loaded (Figure 6c):

$$C_1 = C_2 \cong 0, \quad S_1 \cong 0, \quad S_2 \cong 1 \tag{13}$$

$$\omega_1 \cong V/r, \quad \omega_2 \cong 2\omega_m - V/r \tag{14}$$

The second type of traction problem is quite common on RWD cars with a high power-to-weight ratio and/or a weight distribution biased to the front, front-engined cars for instance. Even more so on FWD cars, where the longitudinal load transfer removes vertical load from the front wheels on power. In any case whenever the inner wheel tends to spin, the open differential will prevent saturation of the outer wheel, allowing for the generation of enough lateral force in conjunction with small slip angles, hence restraining power understeer on a FWD car and power oversteer on a RWD car at the expense of traction performance.

F. Torque bias range: spool vs open differential

Two equivalent types of diagrams are used to visualize the differential working range, while a third, simplified type will be presented later on in Fig. 14. The first one (Figure 7a) shows the torque delivered to each drive wheel vs the differential input torque. The second, more popular diagram shows the left vs right output torques (Figure 7b). In both diagrams the first quadrant corresponds to on power operation ($C_m > 0$) while the third one to off power ($C_m < 0$). The lines *AB* (on power) and *CD* (off power) represent the maximum input torque with the equation

$$C_m = C_1 + C_2 \tag{15}$$

while the dotted line *MN* represents the open diff:

$$C_1 = C_2 = C_m/2 \tag{16}$$

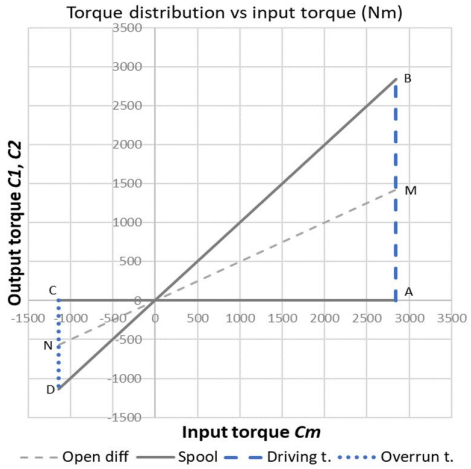

(a)

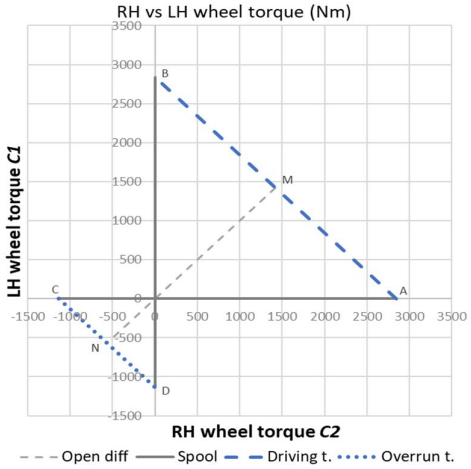

(b)

Figure 7. Torque bias diagrams, spool vs open differential: a) output torque on each wheel vs input torque, b) LH vs RH output torque. Driving and overrun input torques are also shown.

ABDC is the working range of the spool with its typical "butterfly" shape. The torque bias is determined by vertical load and tyre slip and the entire torque can even be delivered to one wheel only. The line *BD* for instance means

$$C_1 = C_m = \Delta C_{MAX} \tag{17}$$

while on the other side (line AC on the first diagram)

$$C_2 = 0 \tag{18}$$

III. THE LIMITED-SLIP OR SELF-LOCKING DIFFERENTIAL

The open differential is suitable for normal road vehicles, while the spool is only compatible with extreme applications [10]. A passive limited-slip differential based on some sort of clutch in parallel with an open differential offers

the potential to cover the entire working range between the open differential and the spool, with the related advantages (and disadvantages): it can be quite effective for high-performance vehicles like sports and racing cars, solving the traction problem and improving vehicle balance and stability at the same time.

The laws describing the open differential are still applicable:

$$\omega_m = \frac{\omega_1+\omega_2}{2} \quad \text{and} \quad C_m = C_1 + C_2 \tag{19}$$

A dissipative device, based on friction, can bypass the differential gears and deliver torque from the faster to the slower wheel output shafts through the differential case, whenever $\omega_1 \neq \omega_2$ (Figure 8a). If $\omega_1 > \omega_2$ for instance:

$$C_1 = C_m/2 - \Delta C \quad \text{and} \quad C_2 = C_m/2 + \Delta C \tag{20}$$

where

$$\Delta C = f(X) \tag{21}$$

is the LSD locking torque, and X can assume different meanings. As stated previously the yaw moment modifying vehicle balance is

$$M_Z = \Delta C \cdot \left(\frac{c}{r}\right) = \Delta F_X \cdot c \tag{22}$$

while the power balance shows that the locking torque is proportional to the power loss through the clutch pack [17]:

$$\Delta C = \left(\frac{W_P}{|\omega_1-\omega_2|}\right) = \left(\frac{W_P}{\Delta\omega}\right) \tag{23}$$

The simplest type of LSD is actually the real-world open differential. The internal friction across the bevel gears can dissipate a certain amount of energy that is sensitive to either input torque and to wheel velocity difference, in a *μ-split* situation for instance.

The two most common types of passive, open differential-based LSD's are described in the following sections, however only the much more complex torque-sensitive, ramp-based differential and the effect of preload are dealt with extensively.

A. Speed-sensitive devices

The locking torque is a function of the angular velocity difference across the differential:

$$\Delta C = f(\Delta\omega) \tag{24}$$

A typical device fitted in parallel with an open differential is the rotary viscous coupling, basically similar to a clutch pack immersed in a silicon fluid (Figures 8b, 9a, and 9b). Its peculiar torque vs velocity curve (Figure 9c) relies on the shear friction of a non-newtonian or pseudoplastic, silicon-based fluid emulsified with air, whose viscosity is sensitive to temperature and pressure variations inside the cartridge as well as to the relative velocity of the alternate disks: torque is transmitted from the faster spinning disks to the slower ones. The design parameters that determine the ΔC vs $\Delta\omega$ curve (Figure 9c) include the viscosity and fill rate of the fluid as well as the geometry and number of discs encapsulated in the unit. The fluid shear frictional resistance curve is also sensitive to ambient temperature.

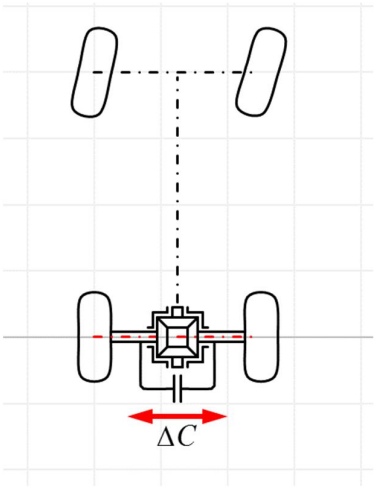

(a)

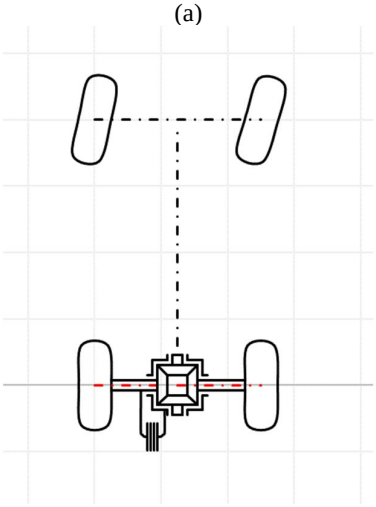

(b)

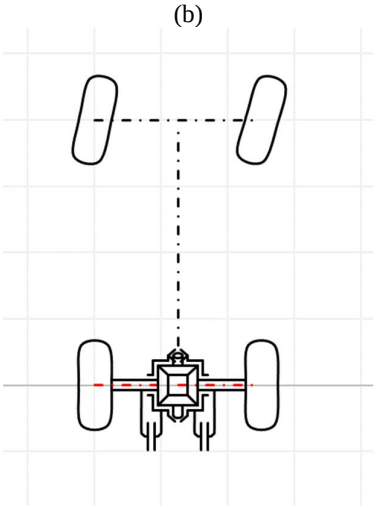

(c)

Figure 8. a) the generic limited-slip differential is composed of a dissipative device in parallel with an open differential, ΔC being the locking torque bypassing the differential itself through the additional device. b) viscous coupling: the locking torque is usually exchanged between the differential case and one output shaft, and transmitted to the other output shaft via the bevel gears. c) ramp differential with double clutch pack: the locking torque is exchanged between the differential case and each output shaft.

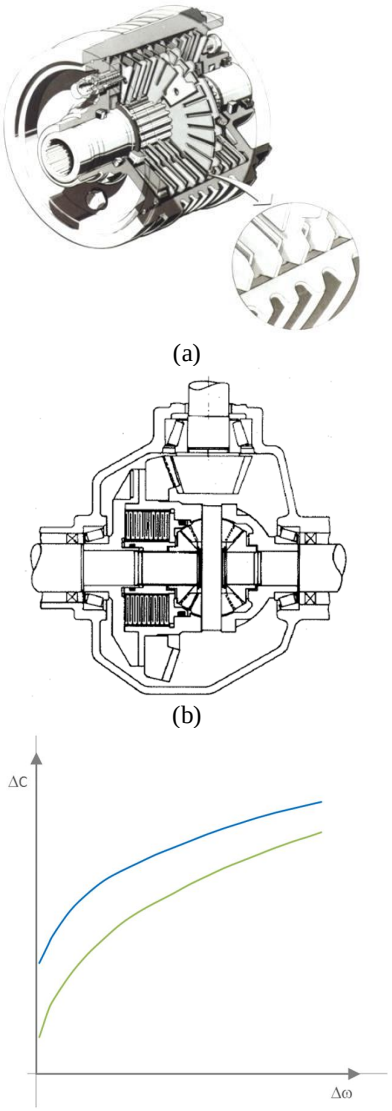

Figure 9. a) viscous coupling, b) in parallel with open diff (courtesy ZF [63]), c) ΔC vs $\Delta\omega$ curve options (from [3]).

Speed-sensitive systems alone can be suitable for vehicle applications in order to deal with the traction problem on low friction surfaces, especially where a smooth intervention is required, such as to prevent "wheel fight" and torque steer on FWD cars, and keep driver workload under control [3,7,10,40,56]. Although a certain preload is always present, just a small amount of torque is transmitted across the differential for low $\Delta\omega$ values in normal driving conditions e.g. in tight corners at low speed and parking maneuvers, therefore the system affects vehicle maneuverability to a very limited extent. For high-performance applications however the degressive curve together with a certain delay in the torque transfer response (building up a speed difference takes time, as stated by [7]) makes this device not very suitable to improve vehicle handling and stability: a very aggressive ΔC vs $\Delta\omega$ curve would be required in this case. More information on viscous couplings for automotive applications can be found in [57,58], while speed-sensitive couplings of the progressive type are dealt with in [7,59].

B. Torque-sensitive devices: a basic model

The locking torque across the differential is proportional to the input torque:

$$\Delta C = f(C_m) \tag{25}$$

The most common torque-sensitive device on road-going sportscars and racing cars is the so-called ramp differential, often known as ZF-type, Salisbury or Hewland Powerflow® differential (Figure 10). In this case the differential case (2) transfers the torque to the satellite gear pins (6) by means of a pair of side rings (11). The torque is exchanged between each pin and a pair of inclined surfaces called ramps (3). The wedging thrust tends to separate the side rings with a contact force proportional to the input torque and the cotangent of the ramp angle σ, pressing them against one or (usually) two wet clutch packs located between each ring and the differential carrier (8 and 9, and Figure 8c), that in turn develop the locking torque. Separate ramp pairs act on and off power, possibly with a different angle (σ = 60° and 30° respectively in Figure 11).

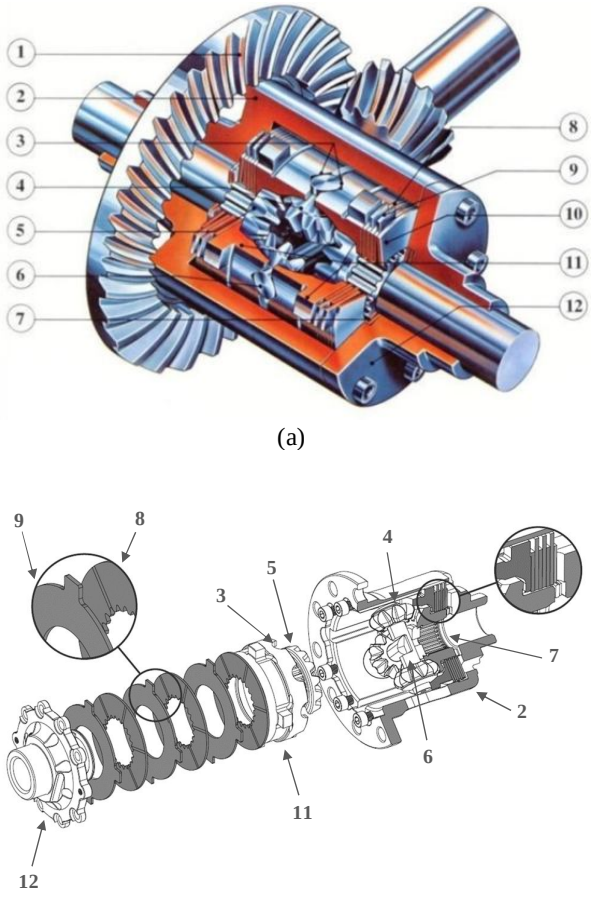

Figure 10. The torque-sensitive ramp differential: internal parts (courtesy ZF [63] and KMP [64]). 1) final drive: crown&pinion, 2) differential carrier, 3) ramp pair on side gear rings (4 at 90°), 4) satellite bevel gears (spider gears), 5) driven bevel gears, 6) satellite gear pin, 7) spline gear, output shaft, 8) clutch disks coupled with output shaft, 9) clutch disks coupled with diff carrier, 10) Belleville spring for axial preload, 11) side gear pressure rings, 12) diff housing cover.

If the number of pin/ramp pairs is 4, as in Fig. 10:

$$N_T = \frac{C_m}{8 \cdot r_{ramp}} \quad \text{with} \quad N_A = N_T \cdot \cot\sigma \tag{26}$$

Assuming that the load distribution is symmetric and considering just one side of the diff, and if the clutch works under uniform pressure distribution, according to standard clutch theory the torque capacity of the clutch pack is

$$C_{clutch} = F_A \cdot \frac{2}{3} \cdot \left(\frac{{R_o}^3 - {r_i}^3}{{R_o}^2 - {r_i}^2}\right) \cdot n \cdot \mu_C$$

with

$$F_A = 4 \cdot N_A = \frac{1}{2} \cdot \left(\frac{C_m}{r_{ramp}} \cdot \cot\sigma\right) \tag{27}$$

where F_A is the axial thrust exchanged between the side gear ring and the clutch pack, R_o and r_i are the outer and inner clutch disc radius respectively, n is the number of clutch face pairs, and μ_c is the uniform clutch friction coefficient.

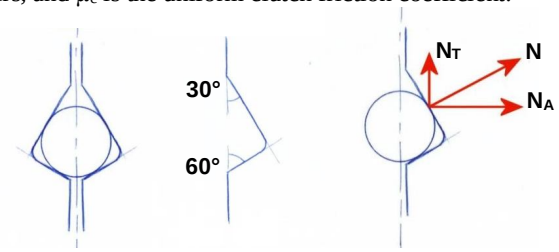

Figure 11. Satellite pin and ramp engagement. Ramp angles: drive 60°, overrun 30°.

The maximum locking torque generated by both clutch packs working under the axial thrust F_A is therefore doubled:

$$\Delta C_{MAX} = \frac{2}{3} \cdot \left(\frac{C_m}{r_{ramp}} \cdot \cot\sigma\right) \cdot \left(\frac{{R_o}^3 - {r_i}^3}{{R_o}^2 - {r_i}^2}\right) \cdot n \cdot \mu_C \tag{28}$$

This type of LSD is a versatile setup tool, especially for racing, as it is separately adjustable on and off power by changing the ramp angles. Also the number of clutch faces, acting as a torque multiplier, can be changed.

The diagrams in Figure 12 are based on a motorsport differential with 45°/30° ramps on and off power respectively and a 6-face wet clutch pack. The working zones are defined by the lines:

On power
line F0 = slower wheel:

$$C_{slowerW} = (C_m + \Delta C_{MAX})/2 \tag{29}$$

line E0 = faster wheel:

$$C_{fasterW} = (C_m - \Delta C_{MAX})/2 \tag{30}$$

Off power
line H0 = slower wheel:

$$C_{slowerW} = -|C_m + \Delta C_{MAX}|/2 \tag{31}$$

line G0 = faster wheel:

$$C_{fasterW} = -|C_m - \Delta C_{MAX}|/2 \tag{32}$$

where the maximum locking torque ΔC_{MAX} is proportional to the input torque C_m. On and off power lines feature different gradients because of the different ramp angles in drive and overrun.

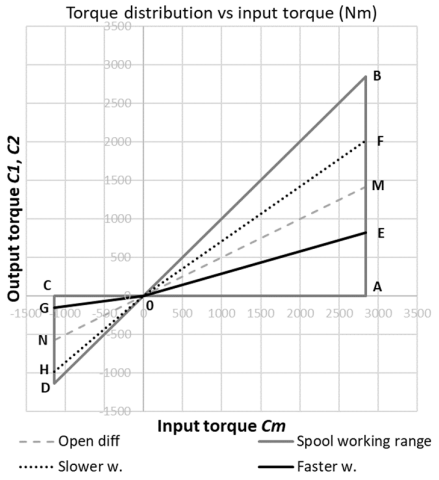

(a)

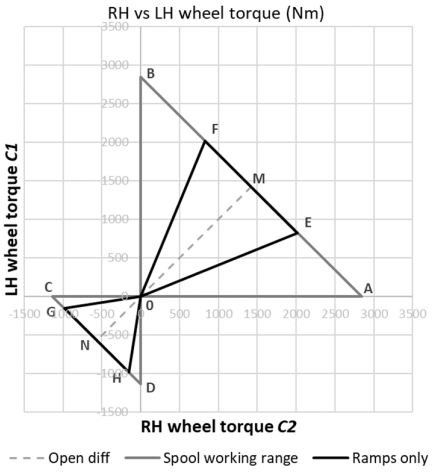

(b)

Figure 12. Torque bias diagrams for a torque-sensitive differential. Engine output torque 500 Nm in fourth gear, diff input torque ≈2800 Nm; overrun torque 200 Nm; ramp angles 45°/30°, no preload, 6 clutch disk face pairs. a) output torque on each side vs input torque, b) LH vs RH output torque.

The Torque Bias ratio can be defined as

$$TB = \frac{C_{slowerW\_MAX}}{C_{fasterW\_MAX}} \tag{33}$$

In this case, with a 60° ramp angle on power (slope of F0 in Figure 12b):

$$TB_{on} = \frac{C_F}{C_E} = 2.45 \tag{34}$$

while the 30° ramp angle generates larger locking torques off power (slope of H0 in Figure 12b):

$$TB_{off} = \frac{C_H}{C_G} = 6.34 \tag{35}$$

The ramp-based, torque-sensitive differential as a matter of fact can be tuned to cover a wide working range between the spool and the free differential: the higher the torque bias ratio, the closer to a spool it becomes as input torque is applied. On the other side as the locking torque is directly proportional to the input torque, the unit is substantially a free differential during cruising and smooth

driving, hence it is also suitable for road car applications. This is however also the main drawback: only limited or null input torque can be delivered on low friction and *μ-split* surfaces, no locking arises and the traction problem occurs.

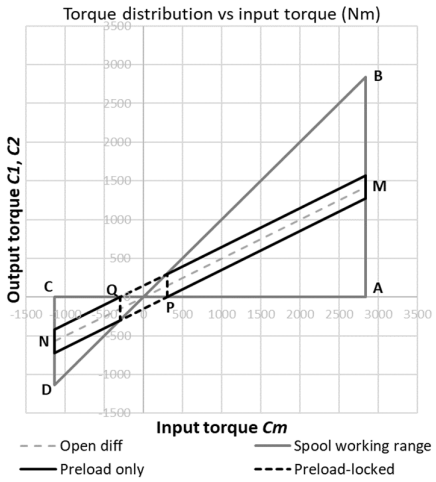

(a)

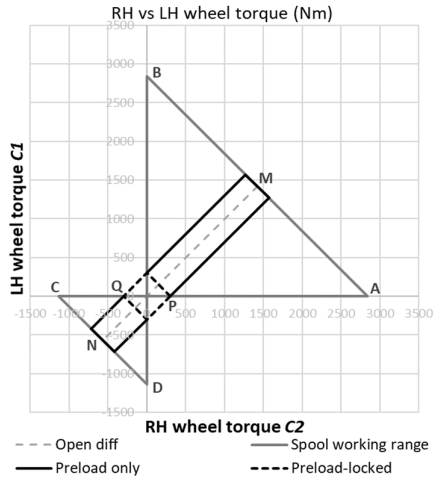

(b)

Figure 13. Torque bias diagrams for preload only. Preload value = 300 Nm.

For the sake of completeness, some vehicle manufacturers used to describe the passive LSD in terms of locking percentage. For example Porsche offered such an option on 911 models in the 80's: it was described as a 40% locking differential, thus featuring symmetrical behaviour on and off power. The locking percentage can be defined as

$$TB\% = \frac{\Delta C_{MAX}}{C_{input}} \tag{36}$$

Intuitively the open differential and the spool feature a locking percentage of 0 and 100% respectively, while in the case of Figure 12 the LSD is clearly not symmetrical:

$$TB\% = \frac{C_F - C_E}{C_F + C_E} = 42\% \text{ on power} \tag{37}$$

$$TB\% = \frac{C_H - C_G}{C_H + C_G} = 73\% \text{ off power} \tag{38}$$

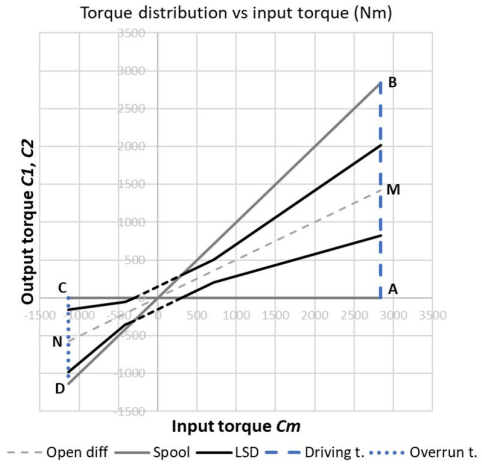

(a)

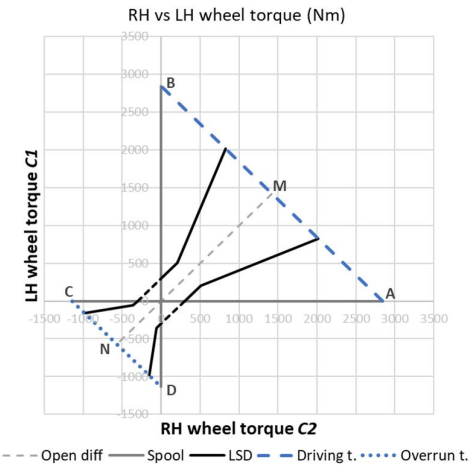

(b)

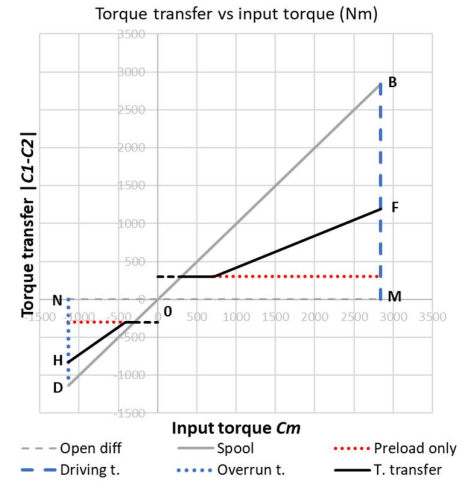

(c)

Figure 14. Combination of preload and ramp effects on the working range of the torque-sensitive differential: ramp angles 45°/30° combined with 300 Nm static preload. a) output torque on each side vs input torque, b) LH vs RH output torque, c) simplified torque bias diagram: torque transfer ΔC vs input torque C_m.

C. The static preload

In order to handle the traction problem an axial preload is often applied statically to the clutch packs e.g. by means of a Belleville spring (no. 10 in Figure 10), resulting in a preload frictional torque across the differential. Points P and Q in Figure 13 correspond to such a preload torque across the differential $\Delta C_{MAX} = P$ which is independent from C_m.

With reference to Figure 13a, for $Q \leq C_m \leq P$ the differential is equivalent to a spool because the input torque is not enough to overcome the preload, while for $C_m < Q$ or $C_m > P$ the input torque C_m has no influence and $\Delta C_{MAX} = P$. The dotted lines in the second and fourth quadrants of Figure 13b define the areas where $C_m = 0$: the input torque can be null during coasting in mid-corner.

It should be stated that the interconnection between left- and right-hand wheels due to preload may interfere with the operation of the ABS therefore high values should be avoided on road cars.

The combination of preload and ramp effects results in a typical shape defined by the ΔC_{MAX} boundaries in Figures 14a and 14b. In addition, a simplified diagram as in [20,22] represents the ΔC_{MAX} working range in terms of ΔC vs C_m (Figure 14c), including the effect of the preload alone.

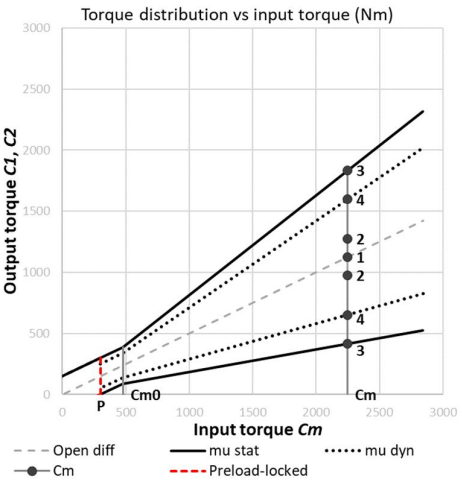

Figure 15. The influence of the friction coefficient.

D. Static and dynamic friction

The transition between static and dynamic friction adds further complexity and can trigger instability of the clutch pack regime in certain conditions. An experimental study of the friction coefficient as a function of relative angular velocity in wet clutch packs can be found in [60], showing the effect of special lubricant additives that can make static friction lower than dynamic friction. The usual assumptions related to friction physics are reversed, enabling smooth operation of automatic transmissions. Some authors assume that a similar friction vs velocity curve is applicable to LSD clutch packs as well: [14,27] for instance. Other sources like [22,61,62] however rely on traditional Coulomb's theory and on Karnopp's modeling, and the authors will do the same, also in agreement with their personal experience on motorsport transmissions. Static and dynamic friction will be considered, with coefficients of μ_S = 0.12 and μ_D = 0.08 respectively [13,66], for a 6-face wet clutch pack. Zooming in the first quadrant of the diagram in Figure 15, for $C_m > 0$ and positive longitudinal acceleration:

As stated above, when $C_m < P$ the input torque is not enough to overcome the static friction preload, that is when $\Delta C \leq C_m$ hence $\Delta C < P$. The differential is fully locked as a matter of fact, and equivalent to a spool.

For $P \leq C_m < C_{m0}$ the preload is still dominating since $\Delta C_{MAX}(C_m) < \Delta C_{MAX}(P)$. The static friction can be exceeded however, a relative angular velocity $\Delta\omega$ will then arise and the maximum preload torque region will stretch from between the solid to the dotted lines.

C_{m0} is the transition between the preload and ramp regions i.e. where the ramp action overcomes the static preload torque. Beyond this point the differential becomes fully torque-sensitive. In fact for a generic input torque $C_m \geq C_{m0}$:

- point 1 corresponds to the condition $C_1 = C_2 = C_m/2$, during acceleration on a straight line on an even road surface for instance. In any case the differential is locked.

- in points 2 the torque is delivered to the wheels in unequal parts but the differential is still locked because $\Delta C = |C_1 - C_2| < \Delta C_{MAX}$.

- points 3 are the limits where $\Delta C = \Delta C_{MAX}$, the differential is unlocked, the dynamic friction coefficient comes into play and the output torque delivery drops to points 4. The areas between the solid and dotted lines on each side are transition zones where clutch pack instability due to stick-slip oscillations can arise, involving driveline torsional dynamics as well.

E. Additional locking effects

An experimental campaign on a dedicated test rig for a motorsport unit is described by Dickason [13], stating that a secondary locking effect should also be taken into account: the axial load applied to the satellite bevel gears is exchanged as wedging force between the gear back spherical face and the side gear rings, resulting into additional thrust on the clutch packs. Locking proportional to input torque is also provided by friction between the same back face and the side rings, and between the bevel teeth. These effects can be taken into account by means of a constant, to be empirically determined: $k \approx 0.08 \div 0.22$.

And finally, taking also the pin/ramp friction coefficient μ_R into account [13,16], (28) can be rearranged as:

$$\Delta C_{MAX} = \\ = C_m \cdot \left[k + \frac{2}{3} \cdot \left(\frac{n \cdot \mu_C}{r_{ramp}} \cdot \frac{\cos\sigma - \mu_R \sin\sigma}{\sin\sigma + \mu_R \cos\sigma} \right) \cdot \left(\frac{{R_o}^3 - {r_i}^3}{{R_o}^2 - {r_i}^2} \right) \right] \quad (39)$$

F. Setup variations

The effects of ramp angle change are shown in Figure 16a. Typical angles ranging from 80° (virtually no locking) to 30° (heavy locking) are usually available in different drive/overrun combinations. The dotted lines show that for a given torque input, ramps larger than 75° on power and 60° off power never manage to overcome the preload.

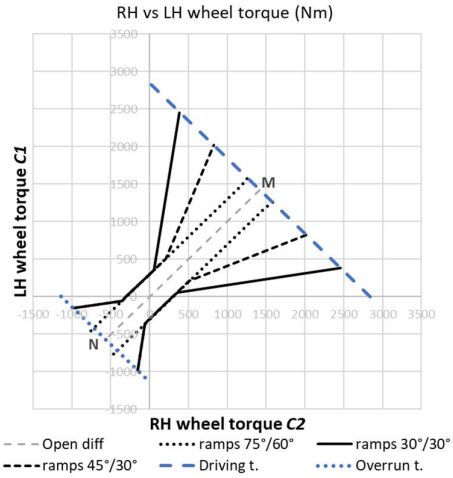

(a)

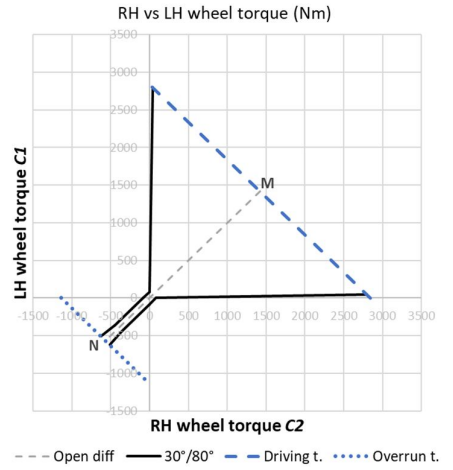

(b)

Figure 16. a) the effect of ramp angle on the torque bias diagrams. Various ramp combinations. As in Figure 12, engine output torque 500 Nm in fourth gear, diff input torque ≈ 2800 Nm; overrun torque 200 Nm; preload torque 300 Nm, 6 clutch disk face pairs. b) same input torque, 30°/80° ramps, preload 80 Nm, 8 clutch disk pairs. TB% on power = 97%, TB% off power = 10%.

Figure 16b shows a somehow extreme example regarding adjustability. Such a setup would probably be unpractical, nevertheless it demonstrates that the locking action can be adjusted to a significant extent, and the whole range between a spool and a free differential can be covered with the standard adjustments. While the differential is virtually free off power (TB% ≈ 0), an aggressive ramp setting on the drive side makes for large torque bias ratios and can even cover the whole quadrant, making the LSD a spool *de facto*, but only on power (TB% ≈ 100%).

Figure 17 shows a real-world example on a single-seater racing car, where the differential allows for some wheel speed difference during turn-in and coasting, but as soon as throttle is applied (around 15%) the wheels are locked together.

The adjustability range allows to address issues like braking and turn-in instability, an inherent problem of racing cars with significant downforce levels due to ground effect; the level of understeer on power can also be tuned by means of the locking action. Care should be taken with the amount of preload built in the differential: too much usually means turn-in and/or mid-corner understeer, not enough might trigger the traction issue in corner exit, with the inner wheel spinning on the wet for instance. This is the reason why externally adjustable preload differentials are used in racing whenever allowed by the regulations.

Figure 17. Time history of the ramp differential action on a racing car. The two lines on the top are the LH and RH rear wheel speeds. The wheel speeds differentiate when the car is approaching the apex. As soon as the driver hits the throttle (bottom arrow) the differential is fully locked (top arrow).

G. Torque-sensitive LSD variants

In top-level systems like the *Hewland EMA*® [65] the preload is adjustable on and off power separately, and can also be negative, see Figure 18. In this case the differential is open for $Q- < C_m < P-$ e.g. when coasting in mid-corner, then the ramp action comes into play and the typical, V-shaped torque-sensitive characteristic is back.

In some special transmissions for motorsport applications like the *Xtrac 379* [66] it is possible to combine a ramp differential (torque-sensitive) with a viscous joint (speed-sensitive) in parallel, in order to obtain a so-called VCP, where low or null static preload values can be used to reduce US in mid-corner coasting. The viscous coupling will take over for traction on low friction surfaces, in the wet for instance. Other types of torque-sensitive LSD's such as the *Torsen*® or the *Quaife ATB*® are based on the separation forces between gears (radial forces for cylinder gears, axial forces for bevel gears) to generate friction and dissipate energy, see [4,11,20].

IV. REAL-WORLD AND SIMULATION EXAMPLES

As anticipated in the introduction, [1] is the only experimental work found by the authors and showing a real-world torque bias diagram. Output torque data have been measured by means of Kistler wheel force transducers on a production-based racing car. The LH vs RH output torque diagram is mapped as a function of longitudinal vehicle acceleration (Figure 19a). The preload is around 400 Nm, and no ramp effect can be seen on overrun.

With regard to the second example, a full GT racing car model was built under supervision of the authors in *VI-CarRealTime*®, a parametric software dedicated to vehicle dynamics, with the aim of performing setup sensitivity

analysis, lap time simulations and DIL/HIL (Driver- or Hardware-in-the-loop) testing on a professional driving simulator [67]. A description of the project is beyond the scope of this work.

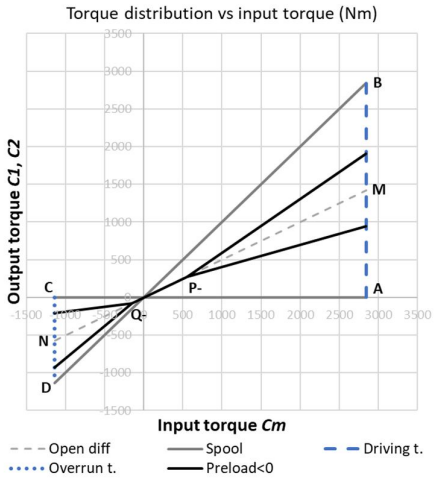

(a)

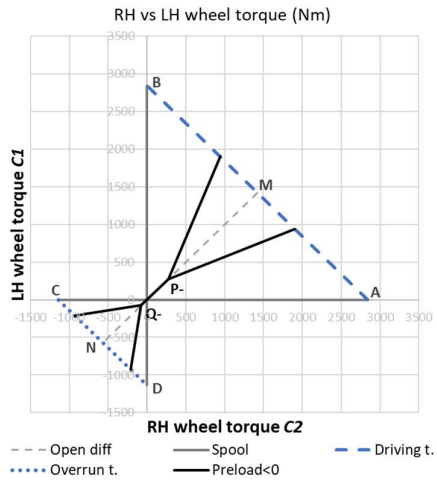

(b)

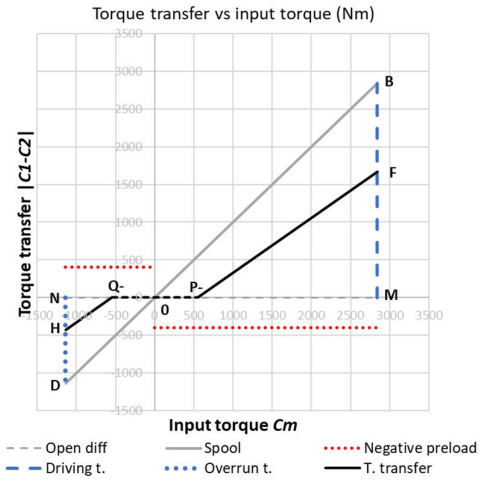

(c)

Figure 18. Torque bias diagrams with negative preload. a), b) standard diagrams, c) simplified torque bias diagram: torque transfer ΔC vs input torque C_m.

Suffice it to say that the model is extremely detailed: tyres are based on flat track experimental data coming from the manufacturer and fitted with Pacejka's Magic Formula 5.2, while aerodynamics is based on wind tunnel maps and it is fully sensitive to ride heights. A validation was carried out successfully with real-world data. The LSD model was built as shown in the previous sections. Figure 19b shows the torque bias diagram for a single lap at the Imola circuit.

The LH vs RH output torque diagram is colour-mapped on input torque. It can be noticed that the whole working zone is used, apart from an "empty" area for low torque input values. The diff acts as a spool quite often, either in the preload and in the ramp regions, and the ramp setting off power is quite aggressive in this case to address braking and turn-in instability.

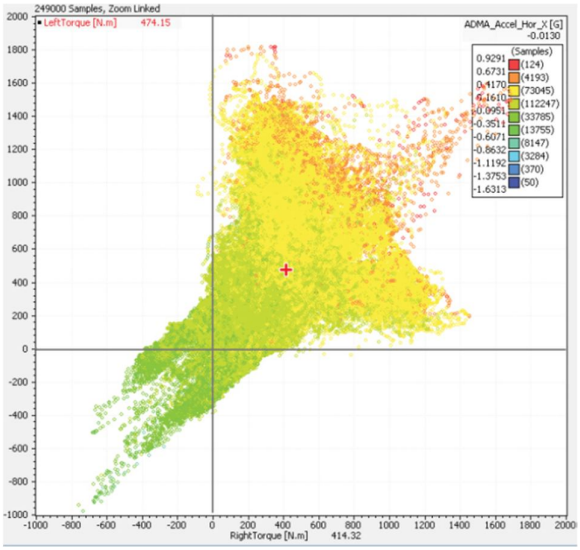

(a)

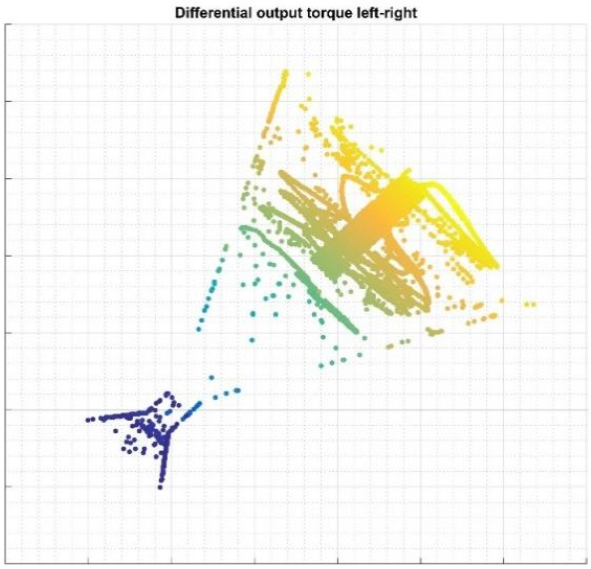

(b)

Figure 19. LH vs RH output torque bias diagrams: a) experimental data based on wheel force transducers, courtesy OptimumG [1]; b) vehicle dynamics model of a GT racing car running at Imola circuit.

V. CONCLUSIONS

Although the subject is well-known in the vehicle dynamics community, the authors felt the need to recap theory and practical aspects related to the limited-slip differential, a passive device used to improve traction capabilities, handling, and ultimately performance of racing cars as well as road-going sportscars.

As a matter of fact the impact of yaw moment control on balance and stability is the focus of attention in literature since active systems became the new standard for vehicle dynamics control. Interestingly enough, the traditional LSD was somewhat a neglected subject in literature and still it is often misunderstood, despite valuable recent research of authors like Tremlett and Hancock.

The present work recaps working principles, advantages and limitations of the passive LSD, with specific focus on the ramp differential, a device that is still the standard even in professional motorsport. A simple model is presented and the torque bias diagram is discussed to an unprecedented level of detail. A comprehensive literature review - from "historic" works on the subject to renowned books to contemporary papers on active yaw control - is also offered in the introduction.

A detailed vehicle dynamics model based on the *VI-CarRealTime*® software is introduced and will be the subject of future research on passive and active limited-slip differentials -on the type of transition between static and dynamic friction for instance- as well as on torque vectoring.

REFERENCES

[1] C. Rouelle, S. Kloppenborg, "Differential Behaviour," *OptimumG lecture notes*, 2016.

[2] R. H. Haas, R. C. Manwaring, "Development of a Limited Slip Differential," *SAE* paper 710610, 1971.

[3] K. Lorenz, C. Dietrich, E. Donges, "Einfluss des sperrdifferentials auf traction und fahrverhalten von fahrzeugen in standardbauweise, teil 1 und 2 (Influence of a limited slip differential on the traction and handling of rear axle driven cars, part 1 and 2)," *AutomobiltechnischeZeitschrift*, 1986, 88(2), 95-100 and (3) 149-153.

[4] S. E. Chocholek, "The development of a differential for the improvement of traction control," *IMechE*, 1988.

[5] M. Okcuoglu, "Adjustable Racing Limited Slip Differentials Utilizing Gerodisc System," *SAE* Technical Paper 962541, 1996.

[6] T. Iwata, T. Murakami, M. Tamura, "Development and analysis of new traction control system with rear viscous LSD," *SAE Transactions*, 1991, 100, 935-945.

[7] H. Huchtkoetter, H. Klein, "The effect of various limited-slip differentials in front-wheel-drive vehicles on handling and traction," *Transmission and Driveline Systems Symposium: Efficiency, Components, and Materials*, Detroit, JAE paper, 1996, 960717, 131-141.

[8] G. Mastinu, E. Battistini, "The influence of limited-slip differentials on the stability of rear-wheel-drive automobiles running on even road with dry surface," *International Journal of Vehicle Design*, 1993, 14 (2/3), 166-183.

[9] W. F. Milliken, D. L. Milliken, "Racecar Vehicle Dynamics," *SAE International*, 1995.

[10] J. C. Dixon, "Tyres, suspension and handling," second edition, *SAE International*, 1996.

[11] P. Wright. "Formula 1 technology," *SAE International*, 2001.

[12] F. Frendo, G. Greco, M. Guiggiani, "Critical review of handling diagram and understeer gradient for vehicles with locked differential," Vehicle System Dynamics, 2006, 44(06), 431-447.

[13] I. Dickason, "Development of a theoretical locking model for a motorsport mechanical plate differential," *Master thesis*, Cranfield University, 2009.

[14] A. J. Tremlett, D. J. Purdy, N. Vaughan, F. Assadian, A. P. Moore, M. Halley, "The influence of torque and speed sensitive differential characteristics in a FWD vehicle during on limit manoeuvres," *Proceedings of FISITA 2012 World Automotive Congress*, Lecture Notes in Electrical Engineering, Beijing, China. Berlin, Heidelberg: Springer, 2012, 193, 79-91.

[15] A. J. Tremlett, D. J. Purdy, N. Vaughan, F. Assadian, A. P. Moore, M. Halley, "The control authority of passive and active torque vectoring differentials for motorsport applications," *Proceedings of the FISITA 2012 World Automotive Congress*, Lecture Notes in Electrical Engineering, Beijing, China. Berlin, Heidelberg: Springer, 2012, 193, 335-347.

[16] A. J. Tremlett, F. Assadian, D. J. Purdy, N. Vaughan, A. P. Moore, M. Halley, "Quasi steady state linearisation of the racing vehicle acceleration envelope: a limited slip differential example," *Vehicle System Dynamics*, 2014, 52(11), 1416-1442.

[17] F. Cheli, "Vehicle Mechanics: differentials and 4-wheel-drive traction," *Lecture notes*, Politechnic of Milan, 2006.

[18] A. J. Tremlett, M. Massaro, D. J. Purdy, E. Velenis, F. Assadian, A. P. Moore, M. Halley, "Optimal control of motorsport differentials," *Vehicle System Dynamics*, 2015, 53(12), 1772-1794.

[19] N. Dal Bianco, R. Lot, M. Gadola, "Minimum time optimal control simulation of a GP2 race car," *Proceedings of the Institution of Mechanical Engineers, Part D: Journal of Automobile Engineering*, 2017, 232(9), 1180-1195.

[20] M. Guiggiani, "The science of vehicle dynamics," Second Edition, Springer, 2018.

[21] E. Bonera, M. Gadola, D. Chindamo, S. G. Morbioli, P. Magri, "On the Influence of Suspension Geometry on Steering Feedback," *Applied Sciences*, 2020, 10(12), 4297.

[22] J. Kinsey, "The advantages of an electronically controlled limited slip differential," *SAE* Technical Paper, 2004, 2004-01-0861.

[23] F. Cheli, F., M. Pedrinelli, F. Resta, G. Travaglio, M. Zanchetta, A. Zorzutti, "Development of a new control strategy for a semi-active differential for a high-performance vehicle," *Vehicle System Dynamics*, 2006, 44(sup1), 202-215.

[24] D. Rubin, S. A. Arogeti, "Vehicle yaw stability control using active limited-slip differential via model predictive control methods," *Vehicle System Dynamics*, 2015, 53(9), 1315-1330.

[25] E. F. Camacho, C. B. Alba, "Model predictive control," *Springer science & business media*, 2013.

[26] Igor S. Nadezhdin, Aleksey G. Goryunov, Flavio Manenti, and Anton O. Ochoa Bike, "Control Systems of a Non-stationary Plant Based on MPC and PID Type Fuzzy Logic Controller," *Lecture Notes in Engineering and Computer Science: Proceedings of The International MultiConference of Engineers and Computer Scientists 2016*, 16-18 March, 2016, Hong Kong, pp219-224.

[27] R. Morselli, R. Zanasi, G. Sandoni, "Detailed and reduced dynamic models of passive and active limited-slip car differentials," *Mathematical and Computer Modelling of Dynamical Systems*, 2006, 12(4), 347-362.

[28] M. J. Hancock, R. A. Williams, E. Fina, M. C. Best, "Yaw motion control via active differentials," *Transactions of the Institute of Measurement and Control*, 2007, 29(2): 137-157.

[29] B. Lenzo, M. Zanchetta, A. Sorniotti, P. Gruber, W. De Nijs, "Yaw Rate and Sideslip Angle Control through Single Input Single Output Direct Yaw Moment Control," *IEEE Transactions on Control Systems Technology*, 2021, 29(1).

[30] M. Hancock, R. Williams, T. Gordon, M. Best, "A comparison of braking and differential control of vehicle yaw-sideslip dynamics," *Proceedings of the Institute of Mechanical Engineers: Part D: Journal of Automobile Engineering*, 2005, 219, 309–27.

[31] K. Sawase, Y. Sano, "Application of active yaw control to vehicle dynamics by utilizing driving/braking force," *JSAE* Rev. 1999, 20, 289–295

[32] H. Sasaki, G. Naitou, Y. Eto, J. Okuda, H. Kusukawa, S. Sekiguchi, "Development of an electronically controlled limited slip differential system," *JSAE* Rev. 1994, 15:348–350.

[33] Y. Ikushima, K. Sawase, "A study on the effects of the active yaw moment control," *SAE* paper 950303, 1995, 425–433.

[34] A. T. Van Zanten, R. Erhardt, G. Pfaff, "VDC, the Vehicle Dynamics Control System of Bosch," *SAE* Technical Paper 950759, 1995.

[35] A. T. Van Zanten, "Bosch ESP Systems: 5 years of experience," *SAE Automotive Dynamics & Stability Conference*, Troy, Michigan (USA), 2000.

[36] A. Mangia, B. Lenzo, E. Sabbioni, "An integrated torque-vectoring control framework for electric vehicles featuring multiple handling and energy-efficiency modes selectable by the driver," Meccanica, 1-20, 2021.
[37] H. Huchtkoetter, T. Gassmann, "Vehicle dynamics and torque management devices," *SAE* Paper 2004-01-1058, 2004.
[38] J. Park, J. Dutkiewicz, K. Cooper, "Simulation and control of Dana's active limited-slip differential e-diff," *SAE* Paper 2005-01-0409, 2005.
[39] D. Piyabongkarn, J. Y. Lew, R. Rajamani, J. A. Grogg, Q. Yuan, "On the use of torque-biasing systems for electronic stability control: limitations and possibilities," *IEEE Trans Control Syst Technol.*, 2007, 15(3), 581–589.
[40] C. Ross, C. Carey, T. Schanz, E. Gaffney, M. Catalano, "Development of an electronically-controlled, limited-slip differential (ELSD) for FWD applications," *SAE* Paper 2007-01-0925, 2007.
[41] F. Assadian, M. Hancock, M. C. Best, "Development of a control algorithm for an active limited slip differential," *In: Proceedings of the 10th International Symposium on Advanced Vehicle Control (AVEC)*, Loughborough (UK), 2008, 55–60.
[42] J. Deur, V. Ivanovic, M. Hancock, F. Assadian, "Modeling and analysis of active differential dynamics," *ASME, J Dyn Syst Meas Control*, 2010, 132.
[43] Ali Momeni, Seyed Reza Moasheri, Hossein Chabok, and Arman Kheradmand, "Developing a Method with an Experimental Study for Estimating Vehicle Speed and Slip using Kalman Filter and Fuzzy Rules," *Lecture Notes in Engineering and Computer Science: Proceedings of The World Congress on Engineering 2015*, 1-3 July, 2015, London, U.K., pp465-470.
[44] M. Abe. N. Ohkubo, Y. Kano, "A direct yaw moment control for improving limit performance of vehicle handling – comparison and cooperation with 4WS," *Vehicle System Dynamics*, 1996, Suppl. 25, 3-23.
[45] M. Canale, L. Fagiano, "Comparing rear wheel steering and rear active differential approaches to vehicle yaw control," *Vehicle System Dynamics*, 2010, 48(05), 529-546.
[46] S. C. Başlamişli, I. E. Köse, G. Anlaç, "Handling stability improvement through robust active front steering and active differential control," *Vehicle System Dynamics*, 2010, 49(5), 657-683.
[47] M. Teraoka, "Development of the electro-magnetic controlled limited slip differential unit (EMCD)," *SAE* paper 931023, 1993, 253–254.
[48] R. De Rosa, M. Russo, R. Russo, M. Terzo, "Optimisation of handling and traction in a rear wheel drive vehicle by means of magneto-rheological semi-active differential," *Vehicle System Dynamics*, 2009, 47(5), 533-550.
[49] G. Gritti, F. Peverada, S. Orlandi, M. Gadola, S. Uberti, D. Chindamo, M. Romano, A. Olivi, "Mechanical steering gear internal friction: effects on the drive feel and development of an analytic experimental model for its prediction," *Proc. of the Intl. Joint Conf. on Mechanics, Design Engineering & Advanced Manufacturing (JCM)*, Catania, Italy, 2017.
[50] C. Benini, M. Gadola, D. Chindamo, S. Uberti, F. P. Marchesin, R. S. Barbosa, "The influence of suspension components friction on race car vertical dynamics," *Vehicle System Dynamics*, 2017, 55(3), 338-350.
[51] F. P. Marchesin, R. S. Barbosa, M. A. L. Alves, M. Gadola, D. Chindamo, C. Benini, "Upright mounted pushrod: the effects on racecar handling dynamics. The Dynamics of Vehicles on Roads and Tracks," *Proceedings of the 24th Symposium of the International Association for Vehicle System Dynamics, IAVSD*, 2016, 543-552.
[52] F. P. Marchesin, R. S. Barbosa, M. Gadola, D. Chindamo, "High downforce racecar vertical dynamics: aerodynamic index," *Vehicle System Dynamics*, 2018, 56(8), 1269-1288.
[53] D. Chindamo, J. T. Economou, M. Gadola, K. Knowles, "A neurofuzzy-controlled power management strategy for a series hybrid electric vehicle," *Proceedings of the Institution of Mechanical Engineers, Part D: Journal of Automobile Engineering*, 2014, 228(9), 1034-1050.
[54] C. Crema, A. Depari, A. Flammini, A. Vezzoli, C. Benini, D. Chindamo, M. Gadola, M. Romano, "Smartphone-based system for vital parameters and stress conditions monitoring for non-professional racecar drivers," *Proceedings of the 2015 IEEE Sensors*, 2015, 7370521.
[55] H. B. Pacejka, "Tyre and vehicle dynamics," *SAE International*, 2012.
[56] M. Gadola, "Lecture notes on self-locking differentials and 4-wheel-drive traction", 2020.
[57] I. H. Taureg, J. Horst, "Induced torque amplification in viscous couplings," *SAE* Paper 900557, 1990.
[58] S. K. Mohan, B. V. Ramarao, "A comprehensive study of self-induced torque amplification in rotary viscous couplings," *J Tribol*, 2003, 125(1), 110-120.
[59] T. Gassmann, J. Barlage, "Visco-Lok: a speed-sensing limited-slip device with high-torque progressive engagement," *SAE* Paper 960718., 1996.
[60] M. Ingram, J. Noles, R. Watts, J. Harris, H. A. "Frictional properties of automatic transmission fluids: Part I – measurement of friction sliding speed behaviour," *Tribol Trans* , 2011, 54(1), 145-153.
[61] M. J. Hancock, "Vehicle handling control using active differentials," *PhD thesis*, Loughborough University, 2006.
[62] J. Deur, J. Asgad, D. Hrovat, "Modelling of CD4E Planetary Gear Set Based on Karnopp Model for Clutch Friction," *Ford Research Laboratories Report No. SRR-2000-0117*, 2000.
[63] Technical Documentation for Limited-Slip Differential, ZF Friedrichsafen AG.
[64] KMP Drivetrain Solutions website, https://www.kmpdrivetrain.com/
[65] Hewland Engineering Ltd, *EMA differential manual*, 2008.
[66] Xtrac Ltd, *379 gearbox manual*, 2005.
[67] Bettinsoli, S. and Leali, G. (2018). Studio e modellazione dinamica di una vettura da competizione Lamborghini Huracán GT3 tramite software VI-CarRealTime. Degree Thesis, University of Brescia.